



Characterization and Development of a Nonlinear Optical Material Imidazolinium Doped With L-Histidine L-Tartrate

B. Deepan Kumar¹, Dr. S. Pullareddy², V.Syamala³, J. Sai Chandra⁴, G. Sujithkumar⁵, K.A. Emmanuel⁶, K.V.L.N Murthy⁷

¹Regional officer, Directorate of technical education, Guindy, Chennai, Tamilnadu, INDIA- 600025.

²Assistant professor. Department of chemistry. Anurag Engineering college, Kodad, Telangana, INDIA. 508206

³Assistant professor. Department of chemistry. Bapatla engineering college. Bapatla. 522101

⁴Dept. of Chemistry, JNTUH University College of Engg. Sultanpur, Telangana, INDIA-502273.

⁵Sri. Ramakrishna mission Vidyalaya college of arts and sciences (Autonomous), Coimbatore, INDIA- 641020.

⁶Dept. of Chemistry Y.V.N.R. Government Degree College, Eluru Dist., A.P. India-521333.

⁷Dept. of Chemistry, SVR Degree college, Macherla, A.P, INDIA- 522426

(Received: 11 June 2024

Revised: 16 July 2024

Accepted: 10 August 2024)

KEYWORDS

dielectric optical studies, powder XRD, Z-scan technique, Imidazolinium L-tartrate

ABSTRACT:

At room temperature, L-histidine-doped IMLT crystalline and imidazolinium L-tartrate (IMLT) crystals produced slowly evaporating crystals. The features of the dopant L-lattice histidine and its capacity to induce high modifications are confirmed by powder x-ray diffraction. The designations of distinct bond configurations present in manufactured crystals are revealed by Fourier transform infrared spectra. The optical dielectric loss of pure and L-histidine-doped IMLT crystals was calculated using dielectric testing. UV-Vis-NIR spectra measurements were used to study the influence of doping on optical properties. The cut-off frequencies of current L-histidine-doped IMLT crystals were 234 and 229 nm, respectively. The structure and surface morphology of pure and L histidine-doped IMLT crystals were peeled away. The carbon-hydrogen-nitrogen (CHN) test is used to determine the amounts of carbon, hydrogen, and nitrogen in pure and L-histidine-doped IMLT crystals. The effects of L-histidine doping in IMLT single crystals. as well as their prevalence in a number of properties of crystals formed in an aqueous solution utilising the slow evaporation method, have been investigated.

I INTRODUCTION

Optical device applications, telecommunications, and data analysis may all benefit from superior-perfection crystals. High-performance nonlinear optical (NLO) materials are employed as parts in frequency conversion techniques, photonic devices, electro optical modulators, and other applications. Organic molecules have more favourable physical features than NLO materials, such as hydrogen bond crystallisation, a strong Van der Waal force, high reflectivity, and a high optical damage threshold for diode lasers. An aromatic heterocyclic compound's

delocalized electron system promotes molecular particularly powerful, which is necessary for improving the crystal's NLO feature.

A p-bonded system exists in the chemical compound imidazole (C₃H₄N₂). Delocalization of electrostatic potential dispersion creates considerable mobility in the electronic structure due to p-orbital overlap. When L-tartaric acid (C₄H₆O₆) and imidazole are mixed, imidazolinium L-tartrate is produced. Second-order NLO substances and stockpiles with a significant dipole moment and a broad transparency range capable of initiating multi-directional hydrogen bond formation (IMLT). Amino acids are deprotonated



carboxylic acids (COO) with a nucleophile amino group (NH₃⁺) that melt at extreme temps.

The host material's dipolar nature promotes resistance to oxidation and clarity, making it an attractive candidate for NLO applications. Asymmetrical carbon atoms are found in almost all amino acids, showing molecular chirality and crystallisation in a non-Centro symmetrical spatial group. The basic, polar amino acid L-histidine (C₆H₉N₃O₂) is doped in IMLT to boost molecule high energy. L-histidine and imidazole have very identical molecular structures. L-histidine, on either side, is an amino acid that has an electron acceptor and people who rely on it, as well as molecular chirality and polyelectrolyte nature, which all amino acids have in common.

The impacts of adding dopants to different crystals have effectively boosted their NLO capabilities. Through a donor-acceptor group, An amino acid enhances the energy dissociation of the parent molecule by causing strong hydrogen bonding. To the parent molecule, the dopants provide improved acentric molecular alignment. Dopants also decrease flaws, fractures, and contaminants by occupying voids or interstitial locations in the parent molecule.

II RELATED WORK

Slow cooling and progressive evaporation processes were used to grow these crystals. In the mother liquor, dopant concentrations ranged from 0.1 to 10 mol present [1-2]. X-ray diffraction (XRD) was used to investigate the pure and doped crystals [2-4]. The LHN crystal has been characterised using single-crystal X-ray diffraction, FT-IR spectra, temperature studies, UV-vis spectra, impact strength, and optical characteristics [5-6]. The novel quick freezing crystallisation approach is being employed for the first time to investigate nucleation management, From pure aqueous system, The well-known amino acid L-forms histidine's were isolated and crystallized[8].

Slow evaporation and variable molar ratios of L-Histidine doped GSN crystals were used to make single GSN crystals from aqueous phase. The high thermal coefficient of solubility is demonstrated through

solubility investigations of formed crystals at various temperatures [9-10]. These dyes were tested to see how they affected the development and characteristics of a single LHB crystal [11]. The lattice characteristics and peak location alterations generated by dopant L-histidine are confirmed by particle x-ray diffraction [12].

Mechanical tests were done on the generated crystal. The created crystal is soft in nature, according to Vicker's Micro hardness examinations [13]. LHA crystals, both pure and doped with metal (La³⁺), are optically transparent single crystals[14].The most frequent method for studying solvent effects on polymorphic crystallisation is ant solvent crystallisation [15].

III PROPOSED METHOD

3.1 Crystal Growth and Material Synthesis

Melt development, slow evaporation, slow chilling, vapour growth, and other methods for producing single crystals exist, however, because of its simplicity and lack of equipment challenges, for the manufacturing of IMLT single crystals, the slow evaporation method was adopted.

The nucleation was noticed after only one day. Over the course of seven days, a number of small crystals grew. Figure 1 shows photographs of the crystals that were obtained. Figure 2 shows an image of the bulk crystals. In lower dopant concentrations, high-quality clear crystals were produced. Higher concentrations of doped crystals may result in fewer occlusions.

3.2 Diffraction of X-rays in Powder

Figure 1 depicts the PXRD patterns that were recorded. The formed crystal's monoclinic crystal structure belongs to the P21 space group. The image depicts a number of planes of reflection, No phase change has occurred, as evidenced by the pattern. There are no extra peaks due to L-histidine doping, indicating that there are no extra peaks. The enhanced crystallinity of the produced crystals is demonstrated by sharp, high, strong peaks.

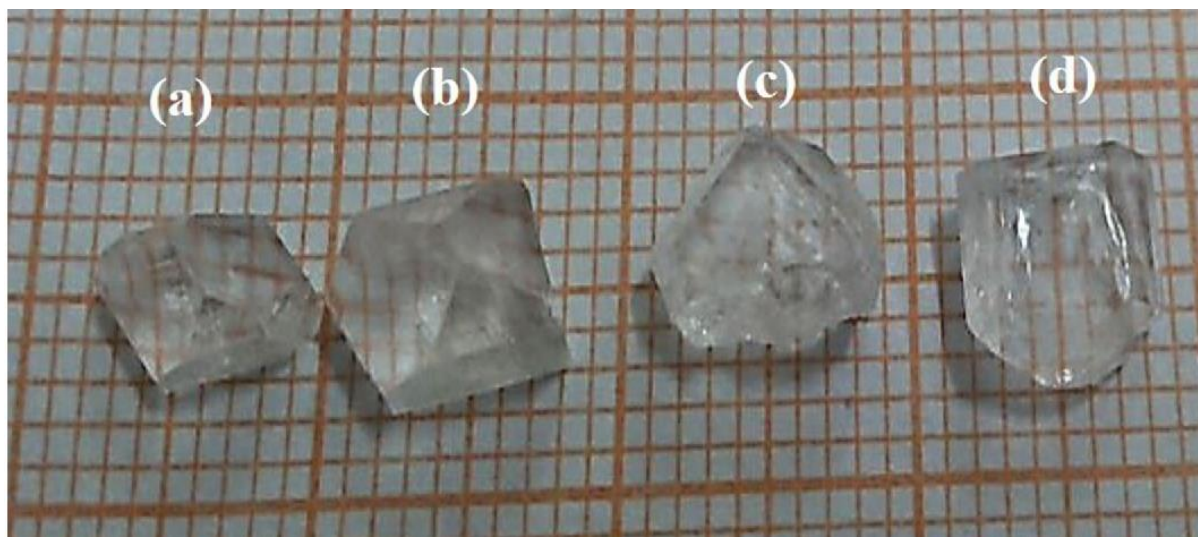


Fig. 1: IMLT crystals with an L-histidine doping (pure IMLT crystals)

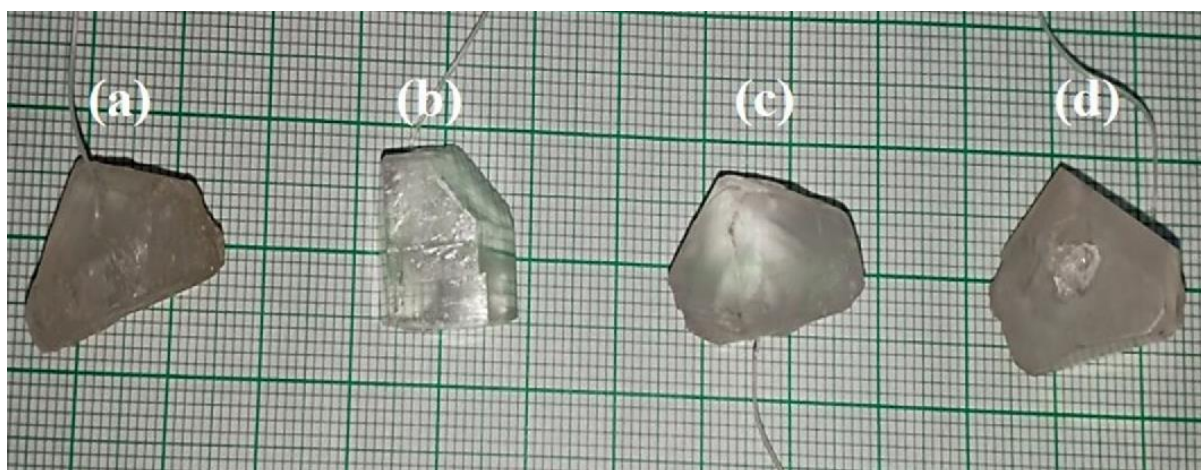


Fig. 2: L-histidine (1 mol), L-histidine (3 mol), and IMLT are all L-histidine derivatives (5 mol).

The temperature, visual, biochemical, and mechanical behaviour of crystals are all limited by crystallinity. The increase in crystallinity of a substance is represented by the size of crystallites. As crystallinity increases, the PXRD pattern's peak grows sharper.

$$D = \frac{K\lambda}{\beta \cos \theta} \quad (1)$$

$$\varepsilon = \frac{\beta \cos \theta}{4} \quad (2)$$

$$\delta = \frac{15\varepsilon}{(a \times D)} \quad (3)$$

where k is the frequency of the x-ray beam, b is the whole breadth at wavelength, K is the Scherer constants, and h is the angle of Bragg's diffraction. When compared to L-histidine-doped IMLT crystals with 3 and 5 mol L-histidine, the 1 mol present L-histidine-doped IMLT crystal had the smallest density (d) and the biggest lattice parameter (see Table II) (D).

3.4 Studies in Optics

The produced crystals are transparent in the UV, optical, and relatively close wavelengths because



electrons travel from the initial state to effects ranging in r-, p-, and n-orbitals.

$$\alpha = -\frac{\ln T}{t} \quad (4)$$

$$\alpha = \frac{\ln I/T}{t} \quad (5)$$

$$\alpha = \frac{-2.303 \log T}{t}$$

(6) T is the absorption, T is the transparency (present), and an is the absorption coefficient, with t being the sample thickness and T being the absorbance (present). The optical electronic properties of the generated crystals were determined using Tauc's figure (Fig. 3) and the relationship.

$$\alpha hv = A(hv - E_g)n \quad (7)$$

Photon energy is represented by hm , a constant is represented by A , the optical energy band gap is represented by E_g , and the typical transition is represented by n . The transition from valance to conduction and valance band might be subtle or overt, and it can even be forbidden.

The following formula for the indirect allowed transition was discovered after rearranging Tauc's plot relation:

$$\alpha hv = A(hv - E_g)^2 \quad (8)$$

$$(\alpha hv)^{1/2} = A(hv - E_g) \quad (9)$$

From $(\alpha hv)^{1/2}$ versus hv , the optical band gap (E_g) values were computed and are also shown.

Table 1: LHA crystals, both pure and doped, yielded XRD data

Parameters of crystal	Pure LHA	LHA with Cu ²⁺	LHA with Mg ²⁺ doping
a(A)	7.843	7.384	7.479
b(A)	8.854	8.244	8.768
c(A)	7.846	7.746	7.874
α	51.75	51.854	51.763
β	76.78	78.53	74.64
γ	81.653	84.63	86.73

The LHA crystal lattice contains Cu²⁺ and Mg²⁺ ions.

3.5 Dielectric Research

Positive ions align in the same direction as the force electromagnetic current when a dielectric substance is exposed to a specific field. Whereas negative ions align in the opposite direction, resulting in polarisation.

$$\frac{Cd}{\epsilon_0 A} = \text{dielectric constant, } \epsilon_r \quad (10)$$

Where C denotes capacitance, ϵ_0 denotes free space permittivity, d denotes crystal thickness, and A denotes crystal surface area. produced crystal dielectric characteristics as a function of wavelength . The following equation can be used to compute dielectric loss ($\tan \delta$).

$$\tan \delta = \frac{\epsilon_n}{\epsilon_0} \quad (11)$$

where $\epsilon_n = \epsilon_r \cdot D$

The dissipation factor D is used to calculate the dielectric loss at different frequencies. It indicates that, As the frequency rises, the electrical resistivity, like the dielectric constant, falls.

IV EXPERIMENTAL RESULT

4.1 X-rays diffraction in a single crystal

The X-ray diffraction of clean, Mg²⁺, and Cu²⁺ doped LHA crystals was studied using the ENRAF NONIUS CAD4-F single X-ray fractal pattern. Table 1 displays the XRD results of pure and doped LHA crystals.

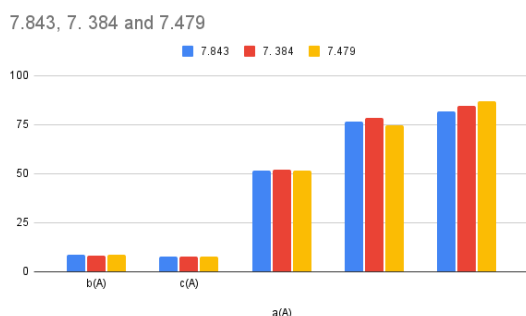


Fig. 3: XRD data of LHA crystals, both doped and undoped

4.2 UV, visible, and near-infrared are examples of spectrum bands.

A Varian portable 5E model dual spectrophotometer was used to assess absorption coefficient between 200 and 2500 nm on these cleaned crystal samples with a thickness of 4–6 mm. The spectra show that LHA crystals, both pure and doped, absorbed between 240 and 1380 nm (Fig. 4). As indicated in the spectra, The cut-off frequencies of pure and doped LHA crystals are lower. Cu²⁺ and Mg²⁺ doped crystals' absorbance has been significantly reduced.

Table 2: Visual representations of produced crystals' crystallite (D), stress (e), and dislocation density (d).

Crystal	Dimensions of crystallites	Strain (ε)	Dislocation density (d)
Pure IMLT	2.745	12.86	19.56
1 mol.% L-histidine	3.856	7.07	12.60
3 mol.% L-histidine	5.742	9.74	17.85
5 mol.% L-histidine	1.632	12.74	16.96

Table II reveals that the 1 mol. present L-histidine-doped IMLT crystal has the least density (d) and the biggest crystallite size when compared to the 3 and 5 mol. percent L-histidine-doped IMLT crystals (D). With 1 mol L-histidine present, the L-histidine-doped IMLT crystal exhibits a unique crystalline feature.

5 mol. present Lhistidine, pure IMLT	298	3.85
--------------------------------------	-----	------

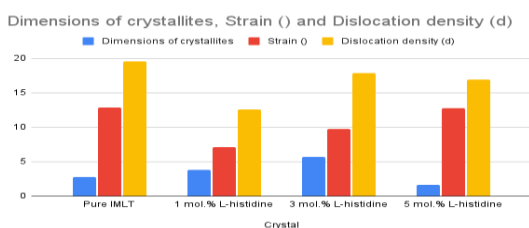


Fig. 4: Formed crystals' crystallite (D), strain (e), and densities (d) are graphically represented.

Table 3: The formed crystals' optical band gap and cut-off wavelength

Crystal	Wavelength cut-off (nm)	Optical band gap E _g (eV)
1 mol. present Lhistidine, pure IMLT	267	3.64
3 mol. present Lhistidine, pure IMLT	284	3.96

The L histidine-doped IMLT crystal with 1 mol% L histidine is noticeably more translucent than the others. As discussed in the PXRD current analysis, the one mole The current L-histidine doped IMLT crystal has a higher crystalline phase than any other crystal ever made. When compared to other formed crystals, there may be a lack of solvent inclusions, which boosts the optical property by minimising scattering centres. Table III shows that the current L-histidine-doped IMLT crystals were 234 and 229 nm, respectively.

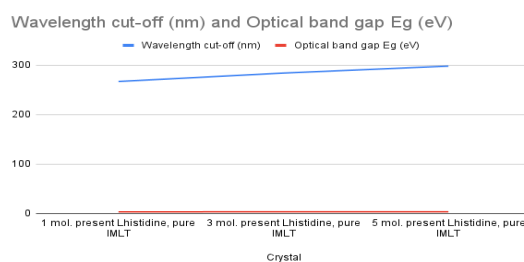


Fig. 5: The produced crystals' cutoff frequency and optical band gap



Imol doping of a single crystal of IMLT In the visible and near-infrared regions, its transparency improves by a factor of ten. Resulting in better optical communication systems. Its usefulness for UV tunable laser applications is shown in Figure 5.

V CONCLUSION

To make pure IMLT and L-histidine-doped IMLT crystals, the researchers used a slow evaporation technique. The cell properties and triclinic crystalline structure of the generated crystals were confirmed by powdered X-ray diffraction. The inclusion of dopant in the crystal lattice is demonstrated by a shift in crystalline structure as doped concentrations increase. The improved characteristics of 1 mol L-histidine-doped IMLT crystalline are determined using the Debye–Scherer method. Maximum displacement and stress were calculated using this technique. The L-histidine-doped crystal with 1 mol% L-histidine looks to be very clear. Spectral analyses in the UV–Vis–NIR range verified this. In a 1 mol L-histidine-doped IMLT crystal, the cut-off frequency is lower. The etching test demonstrates the development and processing of pure and doped IMLT crystals, as well as the EPD decrease in L-histidine doped IMLT crystals containing 1 mol. L-histidine. The current L-histidine-doped IMLT crystal with 1 mol L-histidine outperforms pure and other doped crystals in terms of quality. It is now suitable for usage in NLO systems, according to the results of the characterization investigations.

REFERENCES

1. P. Kumaresan; S. Moorthy Babu; P.M. Anbarasan (2008). *Thermal, dielectric studies on pure and amino acid (l-glutamic acid, l-histidine, l-valine) doped KDP single crystals.* , 30(9), 1361–1368. doi:10.1016/j.optmat.2007.07.002
2. P. Praveen Kumar; V. Manivannan; S. Tamilselvan; S. Senthil; Victor Antony Raj; P. Sagayaraj; J. Madhavan (2008). *Growth and characterization of a pure and doped nonlinear optical l-histidine acetate single crystals.* , 281(10), 2989–2995. doi:10.1016/j.optcom.2008.01.058
3. Pandurangan Anandan; Ramasamy Jayavel (2011). *Crystal growth and characterization of semiorganic single crystals of l-histidine family for NLO applications.* , 322(1), 69–73. doi:10.1016/j.jcrysgro.2011.02.021
4. Yun Zhang; Hua Li; Bin Xi; Yunxia Che; Jimin Zheng (2008). *Growth and characterization of l-histidine nitrate single crystal, a promising semiorganic NLO material.* , 108(2-3), 192–195. doi:10.1016/j.matchemphys.2007.09.006
5. P. Anandan; R. Jayavel; T. Saravanan; G. Parthipan; C. Vedhi; R. Mohan Kumar (2012). *Crystal growth and characterization of l-histidine hydrochloride monohydrate semiorganic nonlinear optical single crystals.* , 34(7), 1225–1230. doi:10.1016/j.optmat.2012.01.042
6. Supriya, Sundareswaran; Sivan, Settu; Srinivasan, Karuppanan (2018). Nucleation Control and Separation of Stable and Metastable Polymorphs of L-histidine Through Novel Swift Cooling Crystallization Process. *Crystal Research and Technology*, (), 1700239–. doi:10.1002/crat.201700239
7. S. Dinakaran, Verma Sunil, S. Das Jerome, Cryst. Eng. Comm. 13 (2011) 2375.
8. Mercina, M., Reena Priya, J., Jayaraman, D., & Joseph, V. (2021). *Synthesis and characterization of Rhodamine B and Methylene Blue doped L - Histidine Bromide single crystals.* *Materials Today: Proceedings.* doi:10.1016/j.matpr.2021.07.272
9. Dhivya, P.; Arun Kumar, R.; Theivasanthi, T.; Vinitha, G.; Kannan, M. D. (2019). *Growth and Characterization of a Nonlinear Optical Material: l-Histidine-Doped Imidazolinium l-Tartrate.* *Journal of Electronic Materials*, (), –. doi:10.1007/s11664-019-07218-2
10. Jayanthi, S. Nalini; Bhuvanewari, N. (2019). AIP Conference Proceedings [AIP Publishing 7TH NATIONAL CONFERENCE ON HIERARCHICALLY STRUCTURED MATERIALS (NCHSM-2019) - Chennai, India (22–23 February 2019)] 7TH NATIONAL CONFERENCE ON HIERARCHICALLY STRUCTURED MATERIALS (NCHSM-2019) - Growth, mechanical, dielectric and



- photoconducting properties of thiourea added L-histidine crystals (TLH). , 2117(), 020020–. doi:10.1063/1.5114600
11. Vijayakumar, A.; Ponnuvel, A.; Kala, A. (2019). Growth and Characterization of Pure and Doped L-Histidine Acetate Crystals. *Materials Today: Proceedings*, 8(), 484–491. doi:10.1016/j.matpr.2019.02.142
 12. Punmalee, Neeranuch; Wantha, Lek; Flood, Adrian E. (2018). Antisolvent Crystallization of Polymorphs of L-Histidine. *Chemical Engineering & Technology*, doi:10.1002/ceat.201700676
 13. Wantha, Lek; Punmalee, Neeranuch; Flood, Adrian E. (2019). Influence of Solvents on Solution-Mediated Polymorphic Transformation of the Polymorphs of L-Histidine. *Chemical Engineering & Technology*, (), ceat.201800699–. doi:10.1002/ceat.201800699